ACS OMEGA

Open Access

http://pubs.acs.org/journal/acsodf

Article

Flow Behavior and Mechanism Insights into Nanoparticle-Surfactant-Stabilized Nitrogen Foam for Enhanced Oil Recovery in the Mature Waterflooding Reservoir

Junchi Lu*

Cite This: *ACS Omega* 2024, 9, 36825−36834

Read Online

ACCESS | Metrics & More | Article Recommendations

ABSTRACT: To solve the problem of poor stability and low enhanced oil recovery efficiency of conventional foam, nanoparticle-surfactant-stabilized nitrogen foam was prepared, and the influence of temperature, salinity, oil content, and pressure on foam performance was systematically investigated. Then, the flow behavior of conventional foam and nanoparticle-surfactant-stabilized foam in porous media was studied. Parallel sand pack flooding and visualization microflooding experiments were performed to investigate the enhanced oil recovery ability of nanoparticle-surfactant-stabilized foam from core-scale to pore-scale. Results showed that the nanoparticles can improve foam performance. When the temperature increases from 60 to 100 °C, the foam volume and foam half-life of nanoparticle-surfactant-stabilized foam decrease by 20 and 36%, respectively. The nanoparticle-surfactant-stabilized foam has a good salt resistance. The oil content limit value of the foam performance is 15%. With the increase of pressure, the foaming performance and foam stability are enhanced obviously. Compared with conventional surfactant-stabilized foam, the nanoparticle-surfactant-stabilized foam can have better plugging and expansion of the swept volume capacity. The micromodel flooding results are consistent with the parallel sand pack flooding results. Compared with conventional surfactant stabilized foam, nanoparticle-surfactant-stabilized foam has better enhanced oil recovery ability than conventional surfactant-stabilized foam due to its higher foaming ability, foam stability, and sweep efficiency improvement ability.

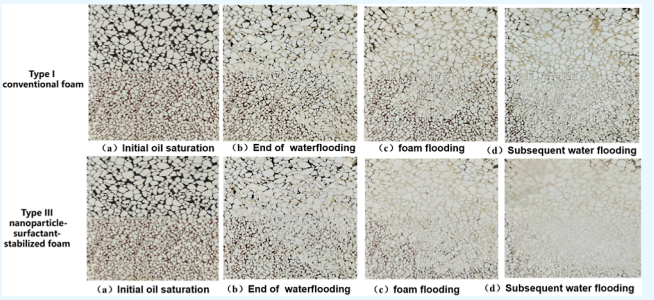

1. INTRODUCTION

Water flooding is considered an important secondary recovery method because it is economically advantageous for oil reservoir development. However, due to the heterogeneity of the reservoir and the adverse mobility ratio between water and oil, the early breakthrough of injected water occurs, and the ultimate oil recovery is about 20−30% of the original oil in place.[1−5] Hence, it is of vital importance to develop more effective techniques to enhance oil recovery in mature water flooding reservoirs. Shengli oilfield has abundant reserves in water flooding development reservoirs. Due to strong reservoir heterogeneity and large differences in water−oil viscosity ratios, the imbalance and contradiction of water flooding are prominent. It faces the problem of a high production fluid volume and high a water−oil ratio, and further technical methods for controlling water and stabilizing oil are urgently needed.

To control water production and increase oil recovery, water shutoff and conformance control technology have been successfully applied in mature waterflooding reservoirs. Different chemical agents, including preformed particle gel, polymer gel, microsphere, and foam, were applied in mature water flooding reservoirs.[6−10] Foam has the advantages of high apparent viscosity and selective water plugging, which have been widely applied in mature water flooding reservoirs. However, for high-temperature and high-salinity reservoirs, the foaming ability and foam stability were not satisfied as expected, which can affect the ability of sweep efficiency to expand and oil recovery ability. Thus, it is of great significance to improve the foam stability to extend the application scope of the foam. In recent years, different foam stabilizers, including polymers, gels, and nanoparticles, have been used. Polymer and gel can enhance the strength of the gas−liquid interface film of the foam and improve its stability. The nanoparticle-stabilized foam has been attracting more and more attention in recent years.[11−31] For surfactant-stabilized foam, the surfactant will dynamically adsorb and desorb at the interface. However, the nanoparticles can adsorb on the gas−liquid interface, and the

Received: June 29, 2024
Revised: August 6, 2024
Accepted: August 9, 2024
Published: August 15, 2024

irreversible adsorption of nanoparticles can increase the surface elasticity of foam and more effectively stabilize foam. In addition, the nanoparticles adsorbed on the interface can block the flow of the liquid phase in the liquid film, delay the thinning of the liquid film, and thus prevent the coarsening and coalescence of the foam. Different nanoparticles, including SiO_2 nanoparticles, TiO_2 nanoparticles, Al_2O_3 nanoparticles, and so on, were used to improve foam stability.[32,33] Besides, the MoS_2 nanosheet and nanoclay were used to stabilize foam.[34,35] It was found that the MoS_2 nanosheet can adsorb on the surface of the foam and extend foam half-life. Although the modified MoS_2 nanosheet can stabilize foam, due to their high cost of its modification, it is not conducive to engineering applications. Thus, among these nanoparticles, due to the cost and foaming stability, the SiO_2 nanoparticle was commonly used as a foam stabilizer to improve foam stability. However, the foaming stability of nanoparticles is lower than that of surfactants; thus, the combination of surfactant and nanoparticles was used to improve the foam performance by utilizing the synergistic effect of surfactant and nanoparticle.[36]

Besides, the commonly used methods for foaming agent evaluation include the Waring Blender method, the airflow method, the Ross−Miles method, etc., but these methods are only used to evaluate the performance of foam under ambient temperature and pressure. However, for the reservoir conditions of high pressure and high temperature, the performance evaluation methods are restricted, which cannot simulate the reservoir pressure and temperature. Thus, it is very crucial to design a high-temperature and high-pressure foam evaluation device to evaluate the foaming ability and foam stability of foaming agents and can better reflect the foam performance under actual reservoir conditions and provide the basis for field application.

Thus, in this study, to solve the problem of poor stability and low enhanced oil recovery efficiency of conventional foam, nanoparticle-surfactant-stabilized novel nitrogen foam was prepared, and the foaming ability and foam stability performance of novel foam were evaluated by using a high-temperature and high-pressure foam evaluation device. The influence of temperature, salinity, oil content, and pressure on foam performance was systematically investigated to clarify the reservoir suitability of foam. Then, the flow behavior of the conventional foam and novel foam in porous media was studied to compare its plugging ability. The enhanced oil recovery ability of conventional foam and novel foam was investigated from core-scale to pore-scale, which can provide mechanism insights into the nanoparticle-surfactant-stabilized nitrogen foam for enhanced oil recovery in a mature water flooding reservoir.

2. MATERIALS AND METHODS

2.1. Materials. The experimental oil was prepared by blending actual crude oil and kerosene from Shengli Oilfield with a viscosity of 35.7 mPa·s at a temperature of 80 °C. The salinity of the simulated formation brine is 20 000−100 000 mg·L^{-1}. The nitrogen (N_2) with a purity of 99.9% was purchased from the Anqiu Heng'an Gas Plant. Different foaming surfactants, including anionic surfactant MES and anionic surfactant AOS, were purchased from Shandong Yousuo Chemical Technology Co., Ltd. The chemical structure formulas of AOS and MES are as follows: AOS: RCH = $CH(CH_2)_n$−SO_3Na, R = C_{14} ∼ C_{16}. MES: RCH(SO_3Na)-$COOCH_3$, R = C_{14} ∼ C_{16}. The nanoparticle foam stabilizer was colloid silica provided by Shengli Oilfield. The colloid silica has a negative charge and hydrophilicity. The median particle size of colloid silica is 15 nm. The visualization glass-etched micromodel was designed and prepared by laser etching according to the pore network model picture from the actual core. The size of the glass-etched micromodel was 4 cm × 4 cm, and the pore size ranged from 50 to 300 μm.

2.2. Methods. *2.2.1. Performance Evaluation of Nanoparticle-Surfactant-Stabilized Nitrogen Foam.* The foaming ability and foam stability performance of foam were evaluated by using the high-temperature and high-pressure foam evaluation device depicted in Figure 1. The blender evaluation foaming method was adopted to obtain the foam volume, half-life of foam, and foam composite index parameters. The specific experimental procedures are as follows: ① The 100 mL foaming agent prepared with the simulated formation brine was first poured into the foam evaluation device. ② Then the nitrogen was injected into the device, and the required pressure was set to simulate the reservoir pressure. ③ Then, the rotating speed was set at 1000r·min^{-1}. The foam volume and half-life of the foam were recorded to obtain the foam composite index parameter. The foam volume V_{max} is defined as the maximum volume of generated foam. The half-life of the foam is defined as the time required for the foam volume to decrease to half of its original volume. Then, the foam composite index parameter was calculated according to the following equation as follows

Figure 1. Performance evaluation process of a high-temperature and high-pressure foam device.

$$F_q = \frac{3}{4} V_{max} t_{1/2} \quad (1)$$

2.2.2. Flow Behavior Evaluation of Foam in Porous Media. The flow behavior of foam was evaluated by conducting sandpack flooding experiments. The experimental procedures were as follows: (1) The sandpack (φ2.5 cm × 50 cm) was prepared by using different mesh quartz sand. Then, water flooding was conducted at an injection rate of 1.0 mL·min^{-1} until the injection pressure was stable, and the permeability of the water phase was calculated. (2) Then, the foam slug was injected into the sandpack at an injection rate of 1.0 mL·min^{-1} until the injection pressure was stable again. The gas/liquid ratio of foaming agent and nitrogen is 1:1. (3) Then, the subsequent water flooding was conducted at an injection rate of 1.0 mL·

https://doi.org/10.1021/acsomega.4c06023
ACS Omega 2024, 9, 36825−36834

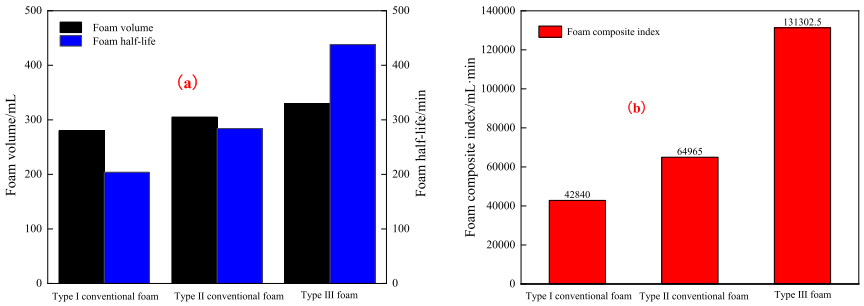

Figure 2. Foam volume, foam half-life, and foam composite index of different type foaming agents: (a) foam volume and foam half-life and (b) foam composite index.

min^{-1} until the injection pressure was stable. (4) The resistance factor (F_r) and residual resistance factor (F_{rr}) were calculated according to the following equation under different conditions.

$$F_r = \frac{\Delta P_{foam}}{\Delta P_{wb}} \quad (2)$$

$$F_{rr} = \frac{\Delta P_{wa}}{\Delta P_{wb}} \quad (3)$$

where ΔP_{foam} is the stable pressure during the foam injection period, MPa, ΔP_{wa}, and ΔP_{wb} are the stable pressure after foam injection during subsequent water flooding and the stable pressure before foam injection during initial water flooding, respectively, MPa.

2.2.3. Parallel Sand Pack Flooding Experiment. The parallel sand pack flooding experiments were conducted to simulate the reservoir heterogeneity and investigate the enhanced oil recovery ability of conventional foam and nanoparticle-surfactant-stabilized nitrogen foam in a heterogeneous reservoir. The experimental procedures were as follows: (1) the high- and low-permeability sand pack was prepared, and the permeability of the water phase was measured. (2) Then, the simulated crude oil was injected into the sandpack until there was no water production. Then, the sandpack was aged for 48 h at 80 °C, and the oil saturation could be calculated. (3) Water flooding period: Then, water flooding was conducted until the water cut reached 98%. (4) Then, the 0.5 PV (pore volume) foam slug was injected into the sandpack, and then the subsequent water flooding was conducted. (5) The water production, oil production, and liquid production were recorded as a function of the injected pore volume. Then, the oil recovery at different periods was calculated to clarify the profile control ability and enhanced oil recovery ability.

2.2.4. Glass-Etching Micromodel Flooding Experiment. In order to better reflect the microscopic seepage and oil displacement characteristics of different types of nitrogen foam at the pore-scale level, the microscopic etching model of complex pore network structure with tortuosity was designed based on scanning to extract the characteristic structure of the rock pore throat. The specific experimental steps are as follows: ① the model was vacuumed and saturated with formation brine and then saturated with simulated oil at 80 °C and aged for 24 h; ② the water flooding process was conducted, and then 2.0 pore volume (PV) foam was injected into the micromodel until no oil was produced. The injection rate was fixed at 0.01 $mL \cdot min^{-1}$. ③ The dynamic flooding process during water flooding and foam flooding was monitored, and the incremental oil recovery was calculated by using image processing software ImageJ to analyze the remaining oil recovery ability.

3. RESULTS AND DISCUSSION

3.1. Subsection. In this study, the foaming ability and foam stability performance of foam were evaluated by using a high-temperature and high-pressure foam evaluation device. First, three different types of foaming agents, including Type I (AOS surfactant), Type II (MES surfactant), and Type III (the combination of MES and colloid silica nanoparticles), were used in this study. Then, the factors influencing the nanoparticle-surfactant-stabilized nitrogen foam were systematically investigated.

3.1.1. Comparison of Foam Performance between Conventional Foam and Nanoparticle-Surfactant-Stabilized Nitrogen Foam. Three different types of foaming agents, Type I (AOS surfactant), Type II (MES surfactant), and Type III (the combination of MES and colloid silica nanoparticle), were used in this study. The concentrations of AOS surfactant and MES surfactant are 0.3%. The formulation and concentration of the Type III foaming agent are a combination of 0.3% MES and 0.1% colloid silica nanoparticles. The foaming performance and foam stability experiments were evaluated under the conditions of a simulated reservoir temperature of 80 °C, pressure of 5 MPa, and salinity of 2×104 $mg \cdot L^{-1}$. Then the differences of foaming and foam stability of different types of foaming agents are compared and analyzed. The experimental results are as depicted in Figure 2.

Under the experimental conditions of a simulated reservoir temperature of 80 °C, pressure of 5 MPa, and salinity of 2×10^4 $mg \cdot L^{-1}$, the foam volume and half-life of different types of foaming agents are significantly different. The highly stable foam formed by the combination of nanoparticles and surfactant has the best foaming ability and the largest foam volume of 410 mL. The foam volume of type II conventional foam (MES surfactant) is 305 mL higher than that of type I conventional foam (AOS surfactant). The half-life of foam is used to evaluate the stability of foam. The longer the half-life, the better the stability of foam. The half-life of nanoparticle- surfactant stabilized foam is the longest, reaching 427 min. Therefore, based on the maximum foam volume and half-life of the foam, the foam composite index of Type III foam (nanoparticle-surfactant-stabilized foam) is nearly 3 times that of type I conventional foam and nearly 2 times that of type II conventional foam. Therefore, based on the foam volume, foam half-life, and foam composite index, nanoparticle-surfactant-stabilized nitrogen foam has the best comprehensive performance, including foaming ability and foam stability.

3.1.2. Influence of Temperature on Foam Performance of Nanoparticle-Surfactant-Stabilized Nitrogen Foam. Type III (the combination of 0.3% MES and 0.1% colloid silica nanoparticles) was used in this part. The foaming performance

https://doi.org/10.1021/acsomega.4c06023
ACS Omega 2024, 9, 36825−36834

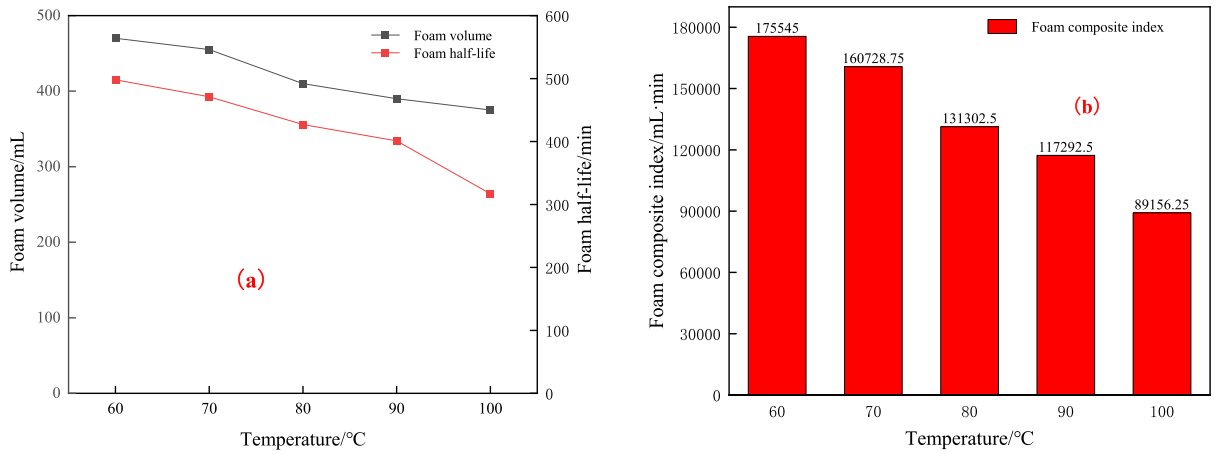

Figure 3. Foam volume, foam half-life, and foam composite index of nanoparticle-surfactant-stabilized nitrogen foam under different temperatures: (a) foam volume and foam half-life and (b) foam composite index.

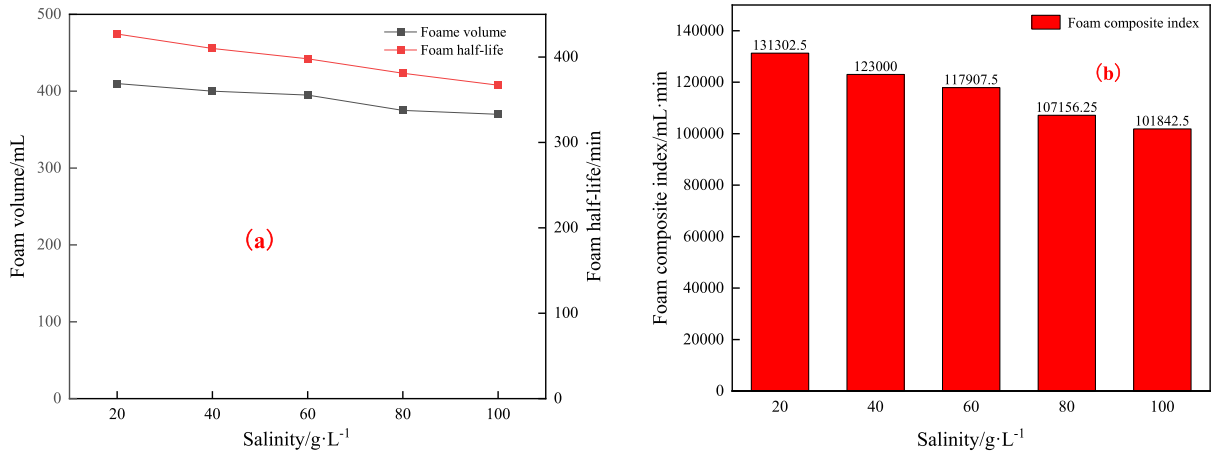

Figure 4. Foam volume, foam half-life, and foam composite index of nanoparticle-surfactant-stabilized nitrogen foam under different salinity: (a) foam volume and foam half-life and (b) foam composite index.

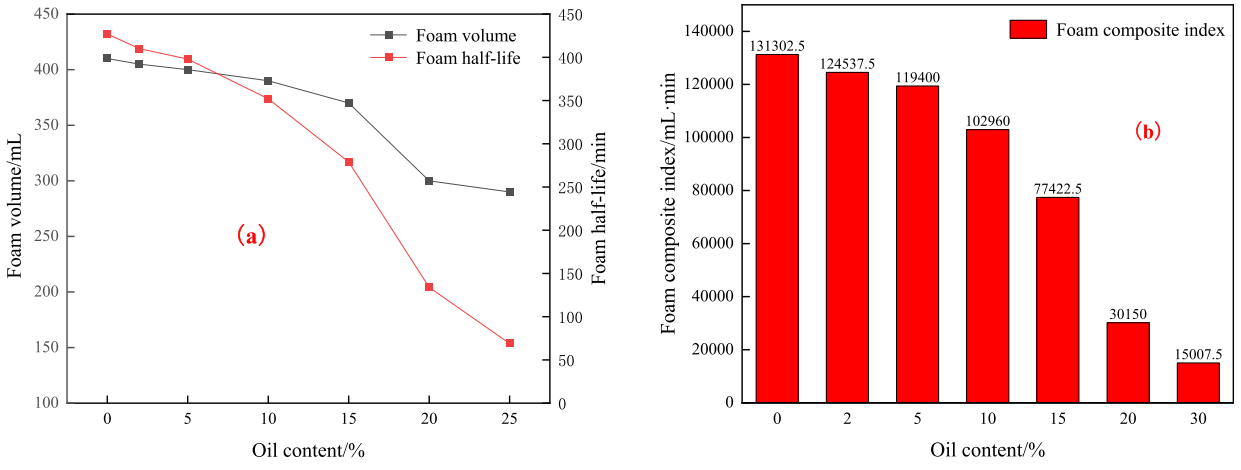

Figure 5. Foam volume, foam half-life, and foam composite index of nanoparticle-surfactant-stabilized nitrogen foam under different oil content: (a) foam volume and foam half-life and (b) foam composite index.

and foam stability experiments were evaluated under different simulated reservoir temperatures ranging from 60 to 100 °C, a pressure of 5 MPa, and a salinity of 2×10^4 mg·L^{-1}. The effect of temperature on the foaming and foam stability of nanoparticle-surfactant-stabilized nitrogen foam is depicted in Figure 3.

With the increase of temperature, the foam volume and foam half-life of the Type III foam (nanoparticle-surfactant-stabilized nitrogen foam) show a downward trend. When the temperature increases from 60 to 100 °C, the foam volume decreases from 470 to 375 mL, and the half-life of the foam decreases from 498 to 317 min. The foam volume and foam half-life decrease by 20

https://doi.org/10.1021/acsomega.4c06023
ACS Omega 2024, 9, 36825−36834

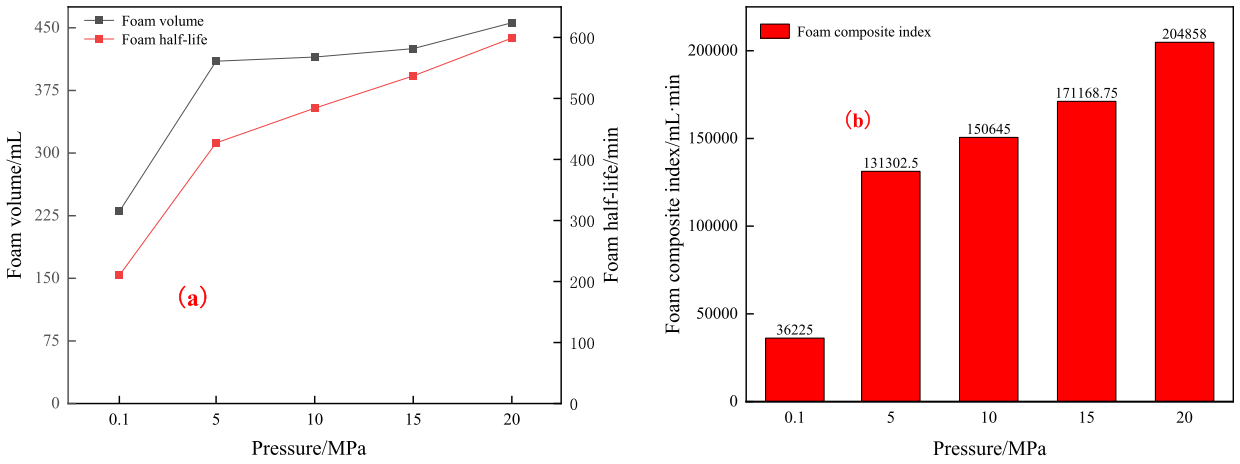

Figure 6. Foam volume, foam half-life, and foam composite index of nanoparticle-surfactant-stabilized nitrogen foam under different pressures: (a) foam volume and foam half-life and (b) foam composite index.

and 36% respectively. Therefore, the effect of the temperature on the foam stability is more obvious. As the temperature rises, the intermolecular force under high temperature conditions is strengthened, resulting in the expansion of foam, the volume becoming larger, and the foam diameter increasing significantly, which intensifies the liquid discharge rate, thus causing the liquid film of foam to become thinner and easier to break and the stability of foam to become worse.

3.1.3. Influence of Salinity on Foam Performance of Nanoparticle-Surfactant-Stabilized Nitrogen Foam. Type III (the combination of 0.3% MES and 0.1% colloid silica nanoparticles) was used in this part. The foaming performance and foam stability experiments were evaluated under the conditions of different simulated salinities ranging from 2×10^4 to 10×10^4 mg·L^{-1}, a temperature of 80 °C, and a pressure of 5 MPa. The effect of salinity on the foaming and foam stability of nanoparticle-surfactant-stabilized nitrogen foam is depicted in Figure 4.

With the increase of salinity from 2×10^4 to 10×10^4 mg·L^{-1}, the foam volume decreases from 410 to 370 mL, and the foam half-life decreases from 427 to 367 min. With the increase of salinity, the foam volume and the foam half-life decrease by 9.8 and 14.1%, respectively. With the increase of salinity, the diffusion double electric layer of the liquid film is compressed, resulting in a reduction in double layer repulsion and a decrease of foam performance, including foaming volume and foam half-life. However, in general, the nanoparticle-surfactant-stabilized nitrogen foam has a good salt resistance.

3.1.4. Influence of Oil Content on Foam Performance of Nanoparticle-Surfactant-Stabilized Nitrogen Foam. Type III (the combination of 0.3% MES and 0.1% colloid silica nanoparticles) was used in this part. The foaming performance and foam stability experiments were evaluated under the conditions of a simulated reservoir temperature of 80 °C, a pressure of 5 MPa, and a salinity of 2×10^4 mg·L^{-1}. The effect of oil content on the foaming and foam stability of nanoparticle-surfactant-stabilized nitrogen foam is depicted in Figure 5.

With the increase of oil content, the foam volume and half-life of the nanoparticle-surfactant-stabilized foam system show a downward trend, but the change trend of the foam volume and half-life of foam can be divided into two stages: slow decline and sharp decline. When the oil content is less than 15%, with the increase of oil content, the foam volume and half-life of foam show a "slow decline" trend with the increase of oil content. When the oil content is less than 10%, the foam volume and half-life are basically unchanged. When the oil content is higher than 15%, the foam volume and the half-life of foam show a "sharp decline" trend. When the oil content increases from 15 to 30%, the foam volume decreases from 370 to 290 mL, and the half-life of the foam decreases from 279 to 69 min. Due to the emulsification of crude oil and foam, small oil droplets enter the foam system, resulting in foam rupture and poor stability. Therefore, for the nanoparticle-surfactant-stabilized nitrogen foam, the oil content limit value of the foaming and foam stability performance is 15%.

3.1.5. Influence of Pressure on Foam Performance of Nanoparticle-Surfactant-Stabilized Nitrogen Foam. Type III (the combination of 0.3% MES and 0.1% colloid silica nanoparticles) was used in this part. The foaming performance and foam stability experiments were evaluated under the conditions of a simulated reservoir temperature of 80 °C, a salinity of 2×10^4 mg·L^{-1}, and a pressure range of 5 to 20 MPa. The effect of pressure on the foaming and foam stability of nanoparticle-surfactant-stabilized nitrogen foam is depicted in Figure 6.

Compared with the ambient pressure of 0.1 MPa and the temperature of 80 °C, the foam volume and half-life of foam are 230 mL and 210 min, respectively, and the foam volume and half-life of foam under high pressure are significantly increased. Under the conditions of high pressure (5−20 MPa) and a temperature of 80 °C, the foam volume and half-life of nanoparticle-surfactant-stabilized foam show an upward trend with the increase of pressure. As the pressure increases from 5 to 20 MPa, the foam volume increases from 410 to 456 mL. Under high pressure, the half-life of foam increases from 427 to 599 min, with the pressure rising from 5 to 20 MPa. The foam composite index of foam increases with an increase of pressure. When the pressure rises, the liquid film and the gas wrapped in it will be compressed, which will reduce the liquid discharge rate and gas diffusion speed of the liquid film. In addition, the foam produced under high pressure is smaller and more uniform, and the foam is more stable. Higher pressure is more conducive to improving the performance of the foam. Therefore, with the increase of pressure, the foaming performance and stability of the foam are obviously enhanced obviously.

3.2. Flow Behavior Evaluation of Foam in Porous Media. The core permeability of the sand pack core is about 3000 mD, the experimental temperature is 80 °C, the gas-liquid

https://doi.org/10.1021/acsomega.4c06023
ACS Omega 2024, 9, 36825−36834

Table 1. Porosity and Permeability of Sand Pack and Experimental Flooding Parameters

test no	foam type	permeability/10^{-3} μm^2	porosity /%	gas−liquid ratio	injection rate/mL·min^{-1}
1	type I conventional foam	3110	37.8	1:1	1.0
2	type II conventional foam	3129	37.2	1:1	1.0
3	type III nanoparticle-surfactant-stabilized foam	3024	38.7	1:1	1.0

Table 2. Stable Pressure During Initial Water Flooding, Foam Injection, and Subsequent Water Flooding Period

test no	foam type	ΔP_{wb}/MPa	ΔP_{foam}/MPa	ΔP_{wa}/MPa	F_r	F_{rr}
1	type I conventional foam	0.0197	0.629	0.246	31.93	12.5
2	type II conventional foam	0.0195	0.769	0.298	39.44	15.28
3	type III nanoparticle-surfactant-stabilized foam	0.0204	1.304	0.756	63.92	37.06

ratio of the foaming agent and nitrogen is 1:1, and the back pressure at the outlet of the core is set to 5 MPa. According to the flow behavior evaluation experimental method for foam in porous media, the flow behavior of different types of nitrogen foam in the same permeability core was studied.

The porosity, permeability of the core, and flooding parameters for specific experiments are shown in Table 1. The stable pressure during water flooding, nitrogen foam flooding, and subsequent water flooding were recorded under the same permeability condition, as shown in Table 2. Then the resistance factor and residual resistance factor of different types of nitrogen foam can be calculated, as depicted in Figure 7.

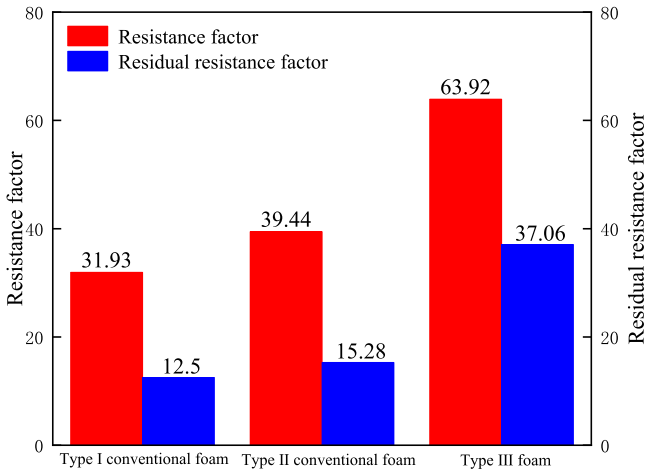

Figure 7. Resistance factor and residual resistance factor of different types of nitrogen foam.

Compared with type I and type II conventional foams, the nanoparticle-surfactant-stabilized foam is higher than type I and type II conventional foam during foam injection and subsequent water flooding. The resistance factor and residual resistance factor of foam are both improved, indicating that the nanoparticle-surfactant-stabilized foam has a higher apparent viscosity and stronger plugging performance. Therefore, the nanoparticle-surfactant-stabilized foam formed by surfactant and nanoparticles has better liquid film strength and apparent viscosity and can have better plugging and expand the swept volume capacity.

3.3. Enhanced Oil Recovery Evaluation of Foam by Parallel Sandpack Flooding Experiments. The parallel sand pack flooding experiments were conducted to simulate the reservoir heterogeneity and investigate the enhanced oil recovery ability of conventional foam and nanoparticle-surfactant-stabilized nitrogen foam in heterogeneous reservoir. The permeability of high and low sandpack cores is 2000 and 500 × 10^{-3} μm^2, and the permeability difference is 4. The experimental temperature is 80 °C, the gas−liquid ratio of foaming agent and nitrogen is 1:1, and the back pressure at the core outlet is set to 5 MPa.

3.3.1. Fraction Flow Analysis of Conventional Foam and Nanoparticle-Surfactant-Stabilized Foam. Figure 8 shows the fractional flow curves of different types of nitrogen. During the initial water flooding stage, the injected water mainly flows through the preferential high-permeability channels, and the percentage of liquid produced by the high-permeability sand pack is significantly higher than that of the low-permeability sand pack. During the foam flooding period, the injected foam will preferentially enter the high-permeability sandpack, and its seepage resistance gradually increases; the percentage of the produced liquid in the high-permeability sand pack decreases and the percentage of the produced liquid of low-permeability sand pack increases, which indicates that the foam can have the profile control ability. During subsequent water flooding, as the injection volume increases, the percentage of produced liquid of the high-permeability sand pack begins to increase at a certain stage, while the percentage of produced liquid of the low-permeability sand pack begins to decrease. It can be inferred that, compared with conventional foam, the nanoparticle-surfactant-stabilized foam has a better sweep efficiency improvement ability than that of conventional surfactant-stabilized foam.

3.3.2. Incremental Oil Recovery Analysis of Conventional Foam and Nanoparticle-Surfactant-Stabilized Foam. Figure 9 depicts the enhanced oil recovery efficiency of conventional foam and nanoparticle-surfactant-stabilized foam. The water flooding oil recovery of different types of foam is in the range of 35.8 to 37.8%. The ultimate oil recovery ranges from 49.75 to 56.7%. The incremental oil recovery ranges from 11.95 to 20.9%. Compared with conventional foam, the nanoparticle-surfactant-stabilized foam has better enhanced oil recovery ability than conventional surfactant-stabilized foam due to higher foaming ability, foam stability, and sweep efficiency improvement ability.

3.4. Micromodel Flooding Efficiency. In order to better reflect the microscopic seepage and oil displacement characteristics of different types of nitrogen foam at the pore-scale level, microscopic visualization flooding experiments were carried out. In this part, two different types of foaming agents, Type I (AOS surfactant) and Type III (a combination of MES and colloid silica nanoparticle), were used in this study. Figure 10 depicts the oil distribution at different periods of Type I conventional foam and Type III nanoparticle-surfactant-stabilized foam. Results show that due to the pore size difference of the model, the injected water mainly flows along the high pore throat flow channel during the water flooding process, resulting in the

https://doi.org/10.1021/acsomega.4c06023
ACS Omega 2024, 9, 36825−36834

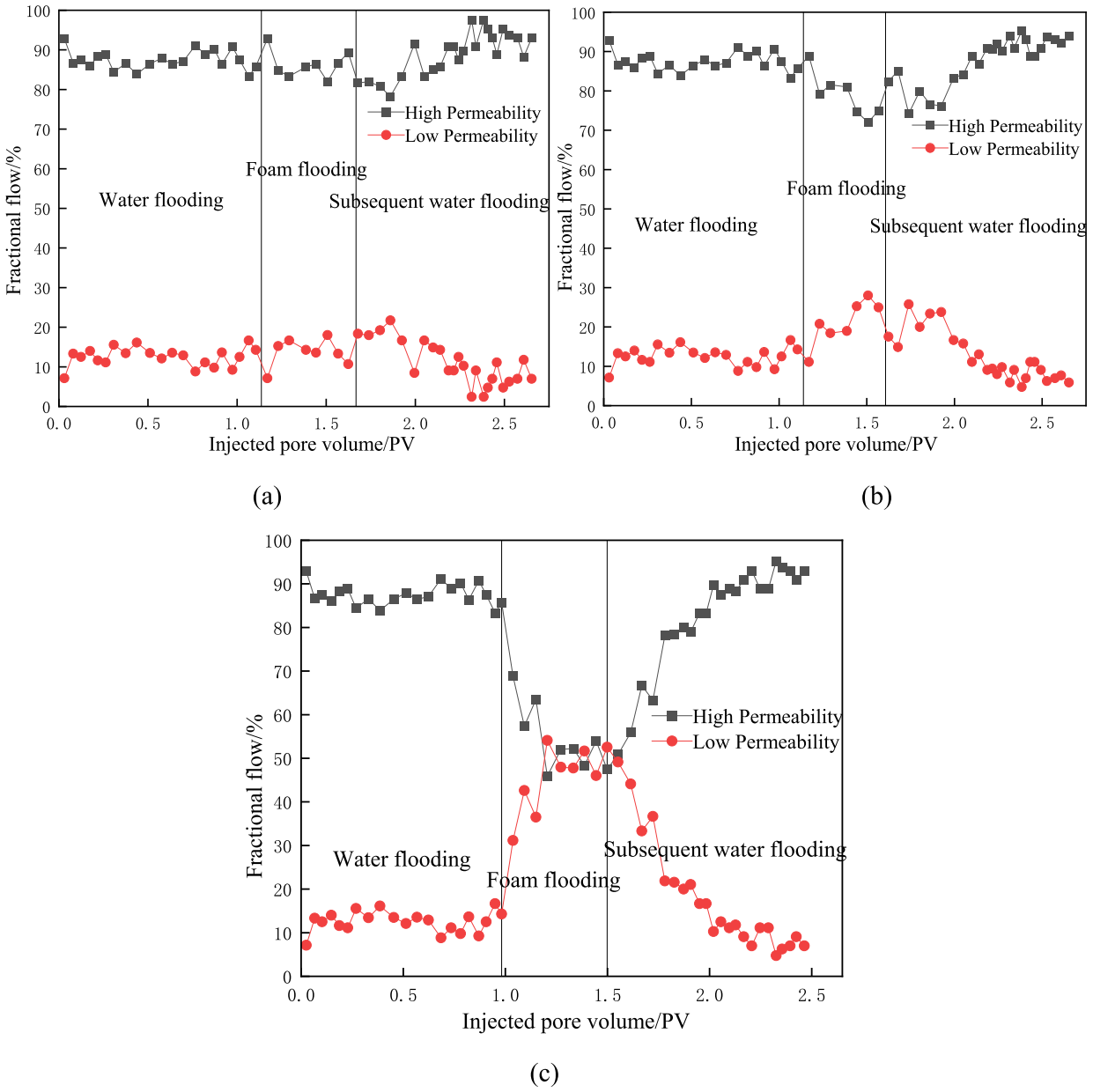

Figure 8. Fractional flow curves of different types of nitrogen foam: (a) type I conventional foam, (b) type II conventional foam, and (c) type III nanoparticle-surfactant-stabilized foam.

remaining oil being unrecovered in the low-permeability area. At the end of water flooding, the water flooding recovery rate is low, and the remaining oil saturation is high.

After injecting type I foam and Type III foam, it can be clearly seen that the foam can change the fluid flow direction and expand the swept volume, which can effectively recover the remaining oil in low-permeability areas of the micromodel. Compared with the Type I foam, the Type III nanoparticle-surfactant-stabilized foam can have a higher expansion of the swept volume. After subsequent water flooding, the remaining oil can be further recovered.

To quantify the oil recovery at different periods and the incremental oil recovery of Type I conventional foam and Type III nanoparticle-surfactant-stabilized foam, the incremental oil recovery was calculated by using the image processing software ImageJ to analyze the remaining oil recovery ability. Figure 11 depicts the incremental oil recovery of Type I conventional foam and Type III nanoparticle-surfactant-stabilized foam. The micromodel flooding results are consistent with the parallel sand pack flooding results. Compared with conventional foam, the nanoparticle-surfactant-stabilized foam has enhance oil recovery ability than conventional surfactant-stabilized foam due to its higher foaming ability, foam stability, and sweep efficiency improvement ability.

4. CONCLUSIONS

In this study, the foaming ability and foam stability performance of different types of foaming agents were evaluated by using a high-temperature and high-pressure foam evaluation device. The influence of temperature, salinity, oil content, and pressure on nanoparticle-surfactant-stabilized nitrogen foam performance was systematically investigated. Then, the flow behavior and enhanced oil recovery ability of different types of foam in

https://doi.org/10.1021/acsomega.4c06023
ACS Omega 2024, 9, 36825−36834

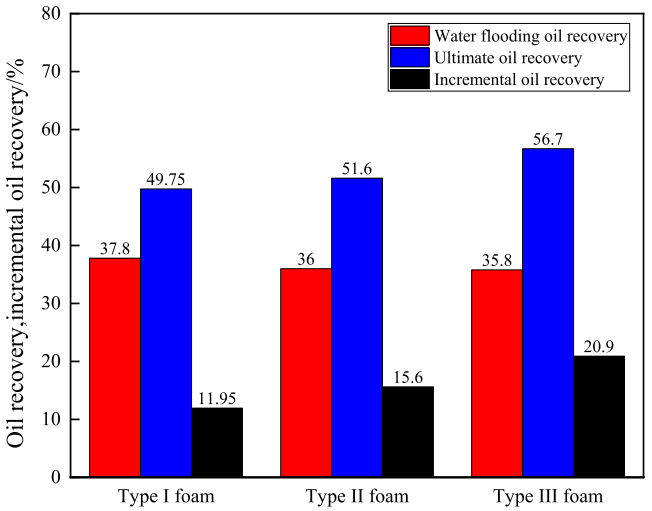

Figure 9. Oil recovery at different periods and the incremental oil recovery of different types of foam.

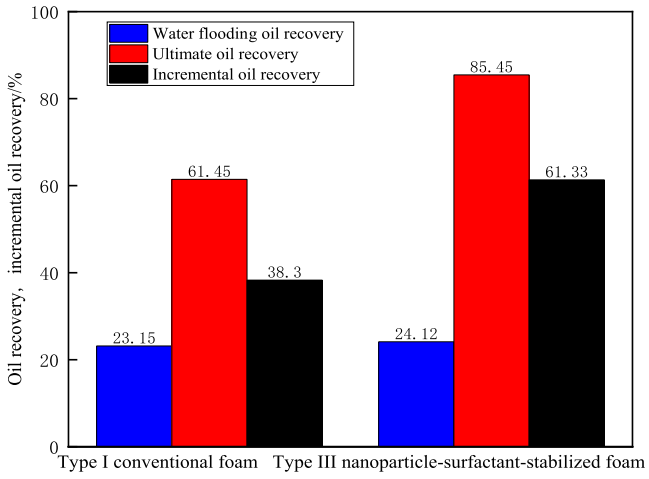

Figure 11. Oil recovery at different periods and incremental oil recovery of Type I conventional foam and Type III nanoparticle-surfactant-stabilized foam.

porous media were investigated from core-scale to pore-scale. The main conclusions could be summarized as follows:

(1) Based on the foam volume, foam half-life, and foam composite index, compared with the conventional foam, nanoparticle-surfactant-stabilized nitrogen foam has the highest foaming ability and the longest foam stability, which can indicate the nanoparticle can improve foam performance in high temperature and saline reservoirs.

(2) When the temperature increases from 60 to 100 °C, the foam volume and foam half-life of nanoparticle-surfactant-stabilized foam decrease by 20 and 36%, respectively. With the increase of salinity from 2×10^4 to 10×10^4 mg·L^{-1}, the foam volume and foam half-life decrease by 9.8 and 14.1%, respectively. The nanoparticle-surfactant-stabilized nitrogen foam has good salt resistance.

(3) When the oil content is less than 15%, with the increase of oil content, the foam volume and foam half-life show a "slow decline" trend, while when the oil content is higher than 15%, the foam volume and foam half-life show a "sharp decline" trend. For the nanoparticle-surfactant-stabilized nitrogen foam, the oil content limit value of the foaming and foam stability performance is 15%. With the increase of pressure, the foaming performance and foam stability are enhanced obviously. Higher pressure is more conducive to improving the foam performance.

(4) Compared with type I and type II conventional foam, the nanoparticle-surfactant-stabilized foam formed by surfactant and nanoparticles has better liquid film strength and apparent viscosity and can have better plugging and expand the swept volume capacity.

(5) The micromodel flooding results are consistent with the parallel sand pack flooding results. Compared with conventional foam, the nanoparticle-surfactant-stabilized foam has better oil recovery ability than conventional surfactant-stabilized foam due to its higher foaming ability, foam stability, and sweep efficiency improvement ability.

AUTHOR INFORMATION

Corresponding Author

Junchi Lu − *College of Mechanical and Vehicle Engineering, Chongqing University, Chongqing 400044, China;* orcid.org/0009-0004-3681-6797; Email: junchilu2024@163.com

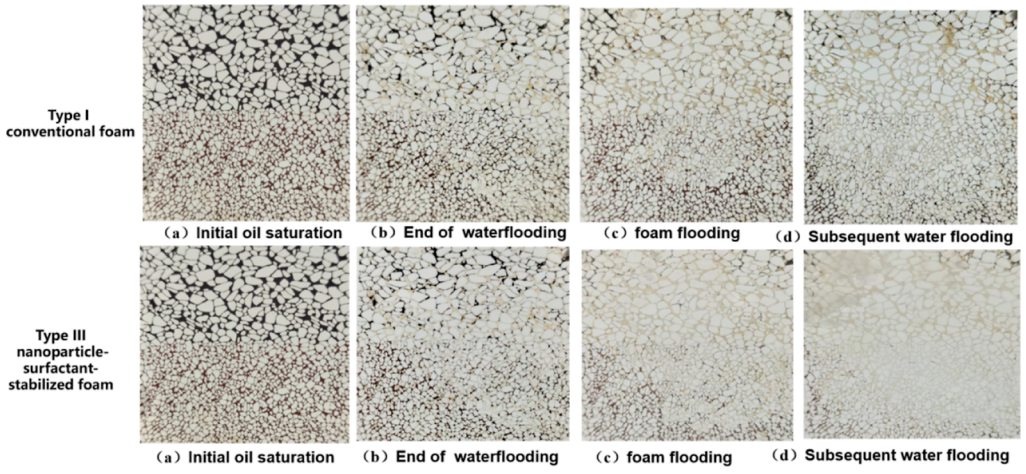

Figure 10. Oil distribution at different periods of Type I conventional foam and Type III nanoparticle-surfactant-stabilized foam.

https://doi.org/10.1021/acsomega.4c06023
ACS Omega 2024, 9, 36825−36834

Complete contact information is available at:
https://pubs.acs.org/10.1021/acsomega.4c06023

Notes

The author declares no competing financial interest.

■ ACKNOWLEDGMENTS

This work was supported by the Exploration and Development Research Institute of Shengli Oilfield, Sinopec. I am grateful to the editors and reviewers for their time and constructive suggestions.

■ REFERENCES

(1) Wang, J.; Feng, Y.; Cao, A.; Zhang, J.; Chen, D. Co-Injection of Foam and Particles: An Approach for Bottom Water Control in Fractured-Vuggy Reservoirs. *Processes* **2024**, *12*, 447.
(2) Yang, J.; Lu, N.; Lin, Z.; Zhang, B.; Zhang, Y.; He, Y.; Zhao, J. Modeling Microscale Foam Propagation in a Heterogeneous Grain-Based Pore Network with the Pore-Filling Event Network Method. *Processes* **2023**, *11*, 3322.
(3) Chen, C.; Xu, H.; Zhang, L.; Li, X.; Zhou, X.; Li, Q.; Wang, P.; Li, M.; Qiu, Y.; Zhang, X.; et al. Foam Systems for Enhancing Heavy Oil Recovery by Double Improving Mobility Ratio. *Processes* **2023**, *11*, 2961.
(4) Gong, Y.; Xin, X.; Yu, G.; Ni, M.; Xu, P. Optimization Study of Injection and Production Parameters for Shallow- and Thin-Layer Heavy Oil Reservoirs with Nitrogen Foam-Assisted Steam Flooding. *Processes* **2023**, *11*, 2857.
(5) Gu, X.; Cai, G.; Fan, X.; He, Y.; Huang, F.; Gao, Z.; Kang, S. Evaluation of Foam Gel Compound Profile Control and Flooding Technology in Low-Permeability Reservoirs. *Processes* **2023**, *11*, 2424.
(6) Ji, Y.; Li, B.; Han, Z.; Wang, J.; Li, Z.; Li, B. Study on Flow Characteristics of Flue Gas and Steam Co-Injection for Heavy Oil Recovery. *Processes* **2023**, *11*, 1406.
(7) Ramezani, R.; Di Felice, L.; Gallucci, F. A Review on Hollow Fiber Membrane Contactors for Carbon Capture: Recent Advances and Future Challenges. *Processes* **2022**, *10*, 2103.
(8) Hu, Y.; Cheng, Q.; Yang, J.; Zhang, L.; Davarpanah, A. A Laboratory Approach on the Hybrid-Enhanced Oil Recovery Techniques with Different Saline Brines in Sandstone Reservoirs. *Processes* **2020**, *8*, 1051.
(9) Wu, Y.; Luo, W.; Jia, X.; Fang, H.; Wang, H.; Yu, S. Application of VES Acid System on Carbonate Rocks with Uninvaded Matrix for Acid Etching and Fracture Propagation. *Processes* **2019**, *7*, 159.
(10) Lv, Q.; Li, Z.; Li, B.; Zhang, C.; Shi, D.; Zheng, C.; Zhou, T. Experimental study on the dynamic filtration control performance of N_2/liquid CO_2 foam in porous media. *Fuel* **2017**, *202*, 435−445.
(11) Niu, Q.; Dong, Z.; Lv, Q.; Zhang, F.; Shen, H.; Yang, Z.; Lin, M.; Zhang, J.; Xiao, K. Role of interfacial and bulk properties of long-chain viscoelastic surfactant in stabilization mechanism of CO_2 foam for CCUS. *J. CO2 Util.* **2022**, *66*, 102297.
(12) Lv, Q.; Zhou, T.; Zhang, X.; Zuo, B.; Dong, Z.; Zhang, J. Enhanced Oil Recovery Using Aqueous CO2 Foam Stabilized by Particulate Matter from Coal Combustion. *Energy Fuels* **2020**, *34*, 2880−2892.
(13) Lv, Q.; Zhou, T.; Zhang, X.; Zheng, R.; Zhang, C.; Li, B.; Li, Z. Dynamic Filtration Behavior of Dry Supercritical CO2 Foam with Nanoparticles in Porous Media. *Ind. Eng. Chem. Res.* **2019**, *58*, 15014−15025.
(14) Lv, Q.; Zhou, T.; Zheng, R.; Zhang, X.; Dong, Z.; Zhang, C.; Li, Z. Aqueous CO_2 Foam Armored by Particulate Matter from Flue Gas for Mobility Control in Porous Media. *Energy Fuels* **2020**, *34*, 14464−14475.
(15) Lv, Q.; Li, Z.; Li, B.; Shi, D.; Zhang, C.; Li, B. Silica nanoparticles as a high-performance filtrate reducer for foam fluid in porous media. *J. Ind. Eng. Chem.* **2017**, *45*, 171−181.
(16) Lv, Q.; Li, Z. M.; Rong, Z. *Study of Ultra-Dry CO2 Foam Fracturing Fluid Enhanced By Graphene Oxide*; International Petroleum Technology Conference: Beijing, China, 2019.
(17) Zhang, Y.; Liu, Q.; Ye, H.; Yang, L.; Luo, D.; Peng, B. Nanoparticles as foam stabilizer: Mechanism, control parameters and application in foam flooding for enhanced oil recovery. *J. Pet. Sci. Eng.* **2021**, *202*, 108561.
(18) Zhao, F.; Wang, K.; Li, G.; Zhu, G.; Liu, L.; Jiang, Y. A review of high-temperature foam for improving steam flooding effect: mechanism and application of foam. *Energy Technol.* **2022**, *10* (3), 2100988.
(19) Issakhov, M.; Shakeel, M.; Pourafshary, P.; Aidarova, S.; Sharipova, A. Hybrid surfactant-nanoparticles assisted CO2 foam flooding for improved foam stability: A review of principles and applications. *Pet. Res.* **2022**, *7* (2), 186−203.
(20) Hosseini-Nasab, S. M.; Zitha, P. L. J. Investigation of chemical-foam design as a novel approach toward immiscible foam flooding for enhanced oil recovery. *Energy Fuels* **2017**, *31* (10), 10525−10534.
(21) Zhang, C.; Wang, P.; Song, G. Study on enhanced oil recovery by multi-component foam flooding. *J. Pet. Sci. Eng.* **2019**, *177*, 181−187.
(22) Liu, P.; Zhang, X.; Wu, Y.; Li, X. Enhanced oil recovery by air-foam flooding system in tight oil reservoirs: Study on the pro-file-controlling mechanisms. *J. Pet. Sci. Eng.* **2017**, *150*, 208−216.
(23) Davarpanah, A.; Mirshekari, B. Numerical simulation and laboratory evaluation of alkali-surfactant-polymer and foam flooding. *Int. J. Environ. Sci. Technol.* **2020**, *17* (2), 1123−1136.
(24) Lang, L.; Li, H.; Wang, X.; Liu, N. Experimental study and field demonstration of air-foam flooding for heavy oil EOR. *J. Pet. Sci. Eng.* **2020**, *185*, 106659.
(25) Rezaee, M.; Hosseini-Nasab, S. M.; Fahimpour, J.; Sharifi, M. New Insight on improving foam stability and foam flooding using fly-ash in the presence of crude oil. *J. Pet. Sci. Eng.* **2022**, *214*, 110534.
(26) Zhang, J.; Di, Q.; Hua, S.; Ye, F.; Li, Y.; Wang, W. Nuclear magnetic resonance experiments on foam flooding and evaluation of foam dynamic stability. *Pet. Explor. Dev.* **2018**, *45* (5), 910−917.
(27) Xu, Z.; Li, Z.; Cui, S.; Li, B.; Chen, D.; Zhang, Q.; Zheng, L.; Husein, M. M. Flow characteristics and EOR mechanism of foam flooding in fractured vuggy reservoirs. *J. Pet. Sci. Eng.* **2022**, *211*, 110170.
(28) Emami, H.; Ayatizadeh Tanha, A.; Khaksar Manshad, A.; Mohammadi, A. H. Experimental investigation of foam flooding using anionic and nonionic surfactants: A screening scenario to assess the effects of salinity and ph on foam stability and foam height. *ACS Omega* **2022**, *7* (17), 14832−14847.
(29) Wen, Y.; Lai, N.; Du, Z.; Xu, F.; Zhang, X.; Han, L.; Yuan, L. Application of orthogonal experiment method in foam flooding system composition and injection parameter optimization. *J. Pet. Sci. Eng.* **2021**, *204*, 108663.
(30) Chen, Z.; Zhao, X. Enhancing heavy-oil recovery by using middle carbon alcohol-enhanced waterflooding, surfactant flooding, and foam flooding. *Energy Fuels* **2015**, *29* (4), 2153−2161.
(31) Wu, Z.; Liu, H.; Pang, Z.; Wu, Y.; Wang, X.; Liu, D.; Gao, M. A visual investigation of enhanced heavy oil recovery by foam flooding after hot water injection. *J. Pet. Sci. Eng.* **2016**, *147*, 361−370.
(32) Xu, Z.; Li, B.; Zhao, H.; He, L.; Liu, Z.; Chen, D.; Yang, H.; Li, Z. Investigation of the effect of nanoparticle-stabilized foam on EOR: nitrogen foam and methane foam. *ACS Omega* **2020**, *5* (30), 19092−19103.
(33) Yekeen, N.; Manan, M. A.; Idris, A. K.; Padmanabhan, E.; Junin, R.; Samin, A. M.; Gbadamosi, A. O.; Oguamah, I. A comprehensive review of experimental studies of nanoparticles-stabilized foam for enhanced oil recovery. *J. Pet. Sci. Eng.* **2018**, *164*, 43−74.
(34) Zheng, W.; Tan, X.; Jiang, W.; Xie, H.; Pei, H. Investigation of nanoclay-surfactant-stabilized foam for improving oil recovery of steam flooding in offshore heavy oil reservoirs. *ACS Omega* **2021**, *6* (35), 22709−22716.
(35) Raj, I.; Liang, T.; Qu, M.; Xiao, L.; Hou, J.; Xian, C. An experimental investigation of MoS2 nanosheets stabilized foams for enhanced oil recovery application. *Colloids Surf., A* **2020**, *606*, 125420.

(36) Singh, R.; Mohanty, K. K. Synergy between nanoparticles and surfactants in stabilizing foams for oil recovery. *Energy Fuels* **2015**, *29* (2), 467−479.

https://doi.org/10.1021/acsomega.4c06023
ACS Omega 2024, 9, 36825−36834